Numerical Investigation of Flow Field of D87 Dual Fuel Engine

A. Gharehghani[1,*] and S. M. Mirsalim[2]

[1]PhD. Student, [2]Assistant Professor, Mechanical Engineering Department, Amirkabir University of Technology, Tehran, Iran.

[*] ayatallah@aut.ac.ir

Abstract

A newly developed heavy duty diesel engine in dual fuel mode of operation has been studied in detail. The main fuel would be natural gas and diesel oil as pilot injection. The importance and effects of mixture preparation and formation through ports, valves and in cylinder flow field with different swirl ratio and tumble on diesel combustion phenomena is an accepted feature which has been studied using a developed CFD model. This analysis is capable to investigate engine geometry, valves lift, valves timing and turbo charging, and its effects on dynamic flow field with variable dual fuel ratio on power and emission levels output. This complete open cycle study of a dual fuel engine has been carried out originally and for the first time and by considering complete grid consisted of four moving valves, two intake ports, two exhaust ports, and the port runners. It is found that important complex flow structures are developed during the intake stroke. While many of these structures decay during the compression stroke, swirl and tumble can survive. The effect of increased swirl ratio at the end of the compression stroke for the D87 engine with a piston bowl is clearly observed in this study. This is important for aiding in good fuel spray atomization. The formation, development, and break-up of tumble flow are seen, contributing to an increase in turbulent kinetic energy at the end of the compression stroke. The complete engine flow field, i.e. the inlet jet, and formation of swirl in the intake ports, is also clearly shown in the study. Results of these simulations assist in the improved understanding of the intake process and its influence on mixture formation and flow field in a dual fuel engine.

Keywords: Dual Fuel, Gas/Diesel engine, Swirl and Tumble Ratio, Flow Field Investigation.

1. INTRODUCTION

The energy consumption and emission is a global issue frequently discussed with different economic, technical and political perspectives. We live in an ever increasing energy consumption which it will certainly grow at least to the 21st century. Today roughly 80% of the world primary energy is supplied by fossil fuels [1]. It is a common belief that these main sources of energy, which is conventional petroleum based liquid fuels, will become scarce for the next generation. Awareness of limitations of fossil fuels reserves and the fact that burning of fossil fuels has a major contribution to the greenhouse gases emission has lead to a growing interest in the use of alternative fuels for internal combustion engines that are known to be the main consumers. Therefore conventional compression or spark ignition engines are converted to run on alternative fuels, such as natural gas, liquefied petroleum gas (LPG) or biogases in power generation, transportation and other applications[2,3]. The main objectives is to improve the combustion process with alternative fuel changes of a conventional internal combustion engines with effective ways to reduce exhaust emissions, without making significant modifications on base engine. Various solutions widely proposed and accepted is the use of natural gas as a substitute for conventional liquid fuel, owing to its Inherent clean nature of combustion with high availability at relatively low prices [4]. It is well

Table1. D87 Engine specification

Engine	4 strokes
Fuel	Methane - diesel oil
Number of cylinder	12
valves per cylinder	4
Bore × Stroke	150 ×180 [mm]
Engine speed	1500 rpm
Compression ratio	11.5:1
Valves timing (same valve timing for two intake valves and two exhaust valves)	IVO 77 BTDC IVC 46 ABDC EVO 77 BBDC EVC 75 ATDC

known that the in-cylinder fluid dynamics in compression ignition engines has an important effect on the fuel distribution, fuel air mixing, ignition delay, and the emissions of the oxides of nitrogen and soot [5, 6]. Various methods are used to investigate these flows, including experimental techniques and numerical simulations [7]. Among these methods, numerical modeling presents a good opportunity to obtain detailed flow information about the entire flow field which may be difficult to obtain with experimental methods. In this paper, mixture formation of air and natural gas through ports and cylinder for a specified dual fuel engine in table 1, is simulated.

2. COMPUTATIONAL PROCEDURE

Open cycle simulation is carried out for mixture formation and combustion process in a dual fuel engine under consideration using KIVA3-V2 CFD. The code is an extension of the earlier KIVA-II, is capable of calculating the processes during transient period for two and three-dimensional chemically reactive fluid flows with sprays where the flow structure could be three dimensional, multi-components with turbulent two-phase reactive flows [8]. This could analyze the combustion processes in internal combustion engines. The code has been modified to calculate the combustion process in dual fuel engine. A CFD code is generated for a 3-D model of inlet, outlet ports and valves including the cylinder itself. Computational grid has been generated using commercial software, ANSYS ICEM CFD [9]. Grid independency has been checked to control the accuracy of results. Initial grid was generated when valves are closed and the piston is at bottom dead center, Figure 1. The blocking and generated mesh by ICEM CFD is presented in Figs. 2 and 3 respectively. Number of cell in the generated mesh is 225000 when geometry is BDC. The mixture formation of natural gas and air which is controlled by swirl ratio has major effect on combustion performance. Swirl ratio is a function of intake valves and ports geometries and its flow interaction with sprayed fuel. The engine combustion is initiated by pilot injection.

A reduced detailed chemical mechanism is considered in KIVA3-V2 code, simulating n-Heptane

Fig. 1. 3-D model at BDC

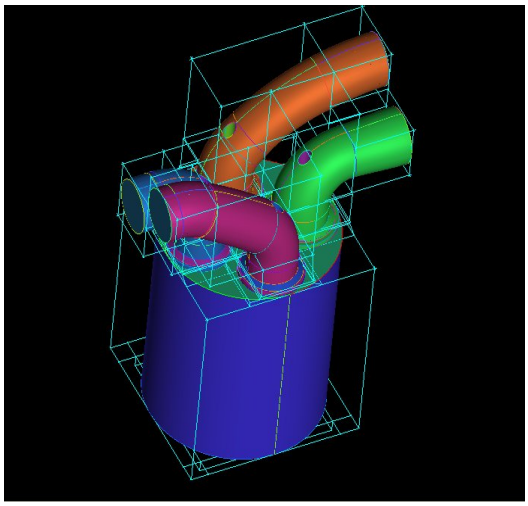

Fig. 2. Blocking generated by ICEMCFD

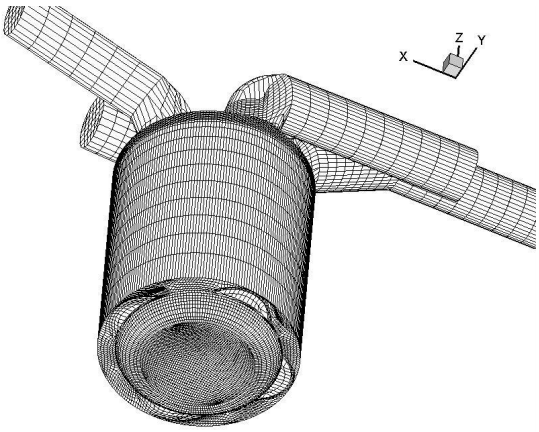

Fig. 3. Computational grid of D87 at BDC

as diesel oil pilot injection and Methane representing natural gas as the main fuel in combustion processes.

The reduction mechanism identifies the species and reaction pathways that are not important; in order to reduce the complexity of mechanisms and the number of variables, yet still to maintain the important features of the full Scheme. The effect of pilot injection on chemical kinetics and its influence on emission level and power output are investigated. Therefore optimization process is carried out for minimum diesel oil pilot injection together with best performance regarding power output and emission level.

3. MODIFIED KIVA-3V CODES TO DUAL FUEL ENGINES

The original KIVA3 model employs for global combustion reaction kinetics and was developed primarily for simulating the performance of conventional engines such as diesel and gasoline engines. To consider dual fuel combustion, the code has been modified to simulate reliably details of the important complex chemical processes leading to initial combustion and its continuation.

The kinetics-controlled reaction rates are usually results in very fast combustion [10, 11] where the fuel, oxidizer and intermediate products may not have enough time to mix down to molecular level in a real engine. The combustion products together with air-fuel mixture may result in the reactions which is partly controlled by the breakup of turbulent eddies that can produce correspondingly a slower reaction rate [12]. In fact both chemical kinetics and turbulence would influence the course of combustion process in real engines which requires suitable models that simulates these interactions [12, 13]. Subsequently a new turbulence-chemistry combustion model which is named partially stirred combustion model is developed [13]. This combustion model was incorporated into the KIVA3V code in the present research.

3. 1. THE GOVERNING EQUATIONS OF GAS PHASE

The KIVA code can be used to solve, both laminar and turbulent flows. The conservation equations for mass, momentum, and energy for above cases differ primarily in the form and magnitude of the transport coefficients, which are much larger for the turbulent case.

The continuity equation for species m is:

$$\frac{\partial \rho}{\partial t} + \nabla \cdot (\rho\ \mathrm{u}) = \nabla \cdot \left[\rho D \nabla \left(\frac{\rho}{\rho} \right) \right] + \dot{\rho}\ + \dot{\rho}\ \delta \qquad (1)$$

Where ρ_m is the mass density of species m, ρ is the total mass density, and u is the fluid velocity. Fick's diffusion law is assumed for a single diffusion coefficient D. The final two terms are source terms due to chemical reaction and spray vaporization. δ is the Kronecker delta function, which is equal to 1 when m=1, and 0 otherwise. By summing Eq. (1) over all species, the total fluid density equation becomes:

$$\frac{\partial \rho}{\partial t} + \nabla \cdot (\rho \mathrm{u}) = \dot{\rho} \qquad (2)$$

The momentum equation for the fluid mixture is:

$$\frac{\partial (\rho \mathrm{u})}{\partial t} + \nabla \cdot (\rho \mathrm{uu}) = -\frac{1}{a} \nabla P - A \quad \nabla \left(\frac{2}{3} \rho k \right) + \nabla \cdot \sigma + F\ + \rho g \qquad (3)$$

Where P is the fluid pressure. The dimensionless quantity, a, is used in conjunction with the Pressure Gradient Scaling (PGS) Method. This is a method for enhancing computational efficiency in low Mach number flows, where the pressure is nearly uniform. A_{tkesw} indicates whether the flow is laminar or turbulent (0 for laminar, 1 for turbulence). σ is the viscous stress tensor, which is given with μ and λ being the first and second coefficients of viscosity, respectively.

$$\sigma\ = \mu \left[\nabla \mathrm{u} + \left(\nabla \mathrm{u} \right) \right] + \lambda \nabla \bullet \mathrm{uE} \qquad (4)$$

The superscript T denotes transpose, and E is the unit dyadic or tensor. μ and λ are the coefficients of viscosity to be defined later. F^s is the rate of momentum gain per unit volume of spray. The specific body force g is assumed to be constant. k is the turbulent kinetic energy.

The internal energy equation is given as follows:

$$\frac{\partial (\rho \mathrm{I})}{\partial t} + \nabla \cdot (\rho \mathrm{uI}) = -P \nabla \cdot \mathrm{u} +$$

$$(1\text{-A} \quad) \sigma : \nabla \mathrm{u} \text{-} \nabla \cdot \mathrm{J} + A \quad \rho \varepsilon + \dot{Q}\ + \dot{Q} \qquad (5)$$

Where I is the specific internal energy, exclusive of chemical energy. ε is the dissipation rate of turbulent

kinetic energy. J is the heat flux vector, which is the sum of contributions due to heat conduction and enthalpy diffusion.

$$J = -K\nabla T - \rho D\sum h \nabla\left(\rho/\rho\right) \quad (6)$$

Where T is the fluid temperature and h_m is the specific enthalpy of species m, and K is the coefficient of heat conduction. The final two terms, $\dot{Q}$ and $\dot{Q}$, are sources due to chemical heat release and spray interaction.

The turbulence quantities (k and ε) that appear in the conservation equation are given by their own transport equation (RNG k-ε equations with some added terms) [14, 17]:

$$\frac{\partial(\rho k)}{\partial t} + \nabla\cdot(\rho u k) = -\frac{2}{3}\rho k(\nabla\cdot u) + \sigma : \nabla\cdot u + \nabla\cdot\left(\frac{\mu}{\Pr}\nabla k\right) - \rho\varepsilon + W \quad (7)$$

$$\frac{\partial(\rho\varepsilon)}{\partial t} + \nabla\cdot(\rho u\varepsilon) = -\left(\frac{2}{3}c - c\right)\rho\varepsilon(\nabla\cdot u) + \nabla\cdot\left(\frac{\mu}{\Pr}\nabla\varepsilon\right) + \frac{\varepsilon}{k}\left[c\,\sigma : \nabla u - c\,\rho\varepsilon + c\,W\right] \quad (8)$$

where W_s is the source term due to the interaction with spray, and the values of constants often used in engine calculation are c_1=1.44, c_2=1.92, c_3=-1.0, c_s=1.5, Pr_k=1.0, Pr_ε=1.3. When the Sub grid Scale (SGS) turbulence model is used, the value of ε is constrained to satisfy the inequality:

$$\varepsilon \geq \left[\frac{c_\mu}{Pr_\varepsilon(c_2 - c_1)}\right]^{0.5}\frac{k^{1.5}}{L_{SGS}} \quad (9)$$

Where L_{SGS} is an input SGS length scale whose value is typically taken to be $4\delta_x$, where δ_x is a representative computational cell dimension. Since $k^{1.5}/\varepsilon$ is proportional to the k-ε length scale (— l is the turbulence length scale), this equation constrains the turbulence length scale to be less than or equal to L_{SGS} and c_μ is a constant whose value is typically 0.09.

4. IN-CYLINDER FLOW

Swirl and tumble are two important parameters controlling in-cylinder fluid rotation. Swirl is organized rotation of the charge about the cylinder axis (Fig. 4) which is created by bringing the intake flow into the cylinder with an initial angular momentum and it's interaction with intake jet/cylinder and wall/piston face. Although many other flow structures generated during the intake process those would decay very quickly but swirl can survive throughout the compression process and even through combustion and expansion processes.

This feature is very useful in enhancing the mixture formation of fuel spray and air with great improvement on combustion process in a CIDI engine. Swirl is generally quantified using a swirl ratio Rs. Swirl ratio is defined as the angular velocity of a solid-body flow rotation ω, which has equal angular momentum to the actual flow which is normalized by the crankshaft angular rotational speed ω.

$$R = \frac{\omega}{\omega} = \frac{\omega}{2\pi N} \quad (10)$$

Where N is the engine speed. The direction of swirl ratio is determined according to the right-hand rule. In KIVA3V code, the swirl ratio is computed on the basis of total angular momentum relative to instantaneous charge mass centre along the cylinder axis and engine speed. The instant centre of mass in the cylinder can be computed as:

$$X = \frac{\sum m x}{M}, Y = \frac{\sum m y}{M}, Z = \frac{\sum m z}{M} \quad (11)$$

Therefore the swirl ratio would be:

$$R = \frac{\sum m\,[v(x - x) - u(y - y)}{I\,\omega} \quad (12)$$

Where xi, yi, and zi are coordinates of vertex, mi is the local vertex mass, M is the instantaneous in-cylinder charge mass, and Iz is total moment of inertia of the air charge relative to instantaneous charge mass

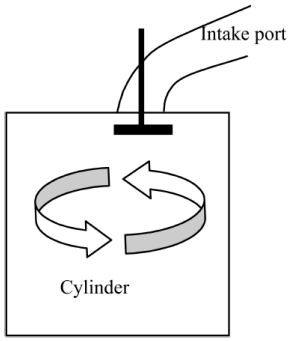

Fig. 4. Formation of Swirl

centre, which can be computed as:

$$I = \sum m\,[v\,(x - x) - u\,(y - y)] \quad (13)$$

Tumble is another important charge motion in cylinder. This is similar to swirl except it is in a vertical plane in the flow field. A tumble flow is usually formed in the later stages during intake stroke and also survives through the compression stroke until the piston approaches to top dead centre. The tumble flow development and relevant break-up is shown in Fig. 5.

Tumble is usually quantified using tumble ratios. In order to get a more complete insight tumble flow pattern, tumble ratio is usually computed in two orthogonal vertical planes, the x–z plane and the y–z plane. The tumble ratios are computed in the same way as swirl, with the exception that the angular momentum and moment of inertia are computed in the two orthogonal vertical planes, that is x–z plane and y–z plane. The tumble ratios TRx and TRy are defined same as swirl ratio:

$$TR = \frac{\omega}{\omega} = \frac{\omega}{2\pi N}, TR = \frac{\omega}{\omega} = \frac{\omega}{2\pi N} \quad (14)$$

Where ω_x and ω_y are the angular velocities of a solid body rotating flow at the y–z and x–z planes which has same angular momentum as actual flow.

So the magnitude of total tumble ratio is:

$$TR = \sqrt{TR + TR} \quad (15)$$

The signs of TRx and TRy are determined according to the right-hand rule.

In KIVA3V code tumble ratios are defined as:

$$TR = \frac{\sum m\,[w\,(y - y) - v\,(z - z)}{I\,\omega} \quad (16)$$

$$TR = \frac{\sum m\,[u\,(z - z) - w\,(x - x)}{I\,\omega} \quad (17)$$

$$I = \sum m\,[(y - y) + (z - z)] \quad (18)$$

$$I = \sum m\,[(x - x) + (z - z)] \quad (19)$$

It is obvious that the flow process in engine cylinder is turbulent. In turbulent flows, the rates of transfer and mixing are several times greater than the rate due to molecular diffusion. Therefore, it is very important to model the turbulence accurately in order to obtain good predictions of physics and chemical processes. The integral scale is a measure of largest-scale structure of the flow field, which is limited in size by the system boundaries, which is:

$$l = C\frac{k}{\varepsilon} \quad (20)$$

Where k and ε are local values from the RNG k- ε turbulence model, C is a model constant, and the turbulent length scale is a mass-weighted cylinder average of this local quantity. The turbulent length scale varies throughout the cycle. At the end of the compression stroke, it is of the order of clearance height [16].

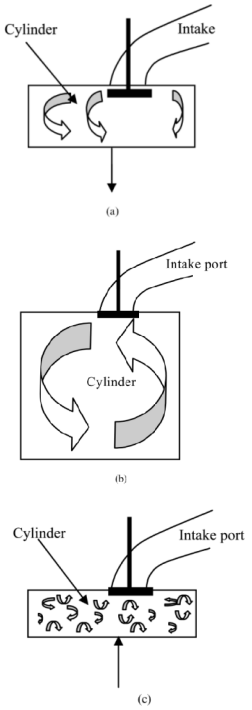

Fig. 5. Formation, development and break-up of tumble during; (a) intake stroke, (b) early compression stroke and (c) late compression stroke

5. INTAKE PROCESS AND IN-CYLINDER FLOW ANALYSIS

Flow details through intake port, valves and in-cylinder flow are investigated in this section and the fuel injection and combustion processes are excluded

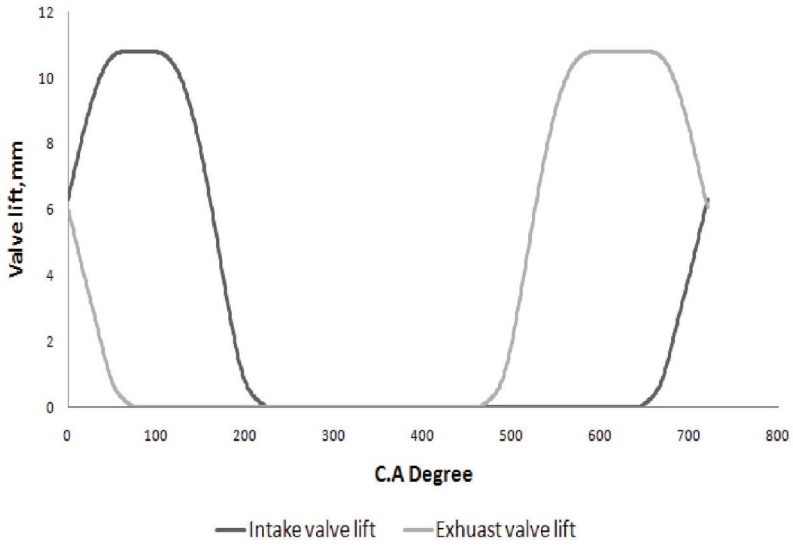

Fig. 6. Valve timing with scavenging

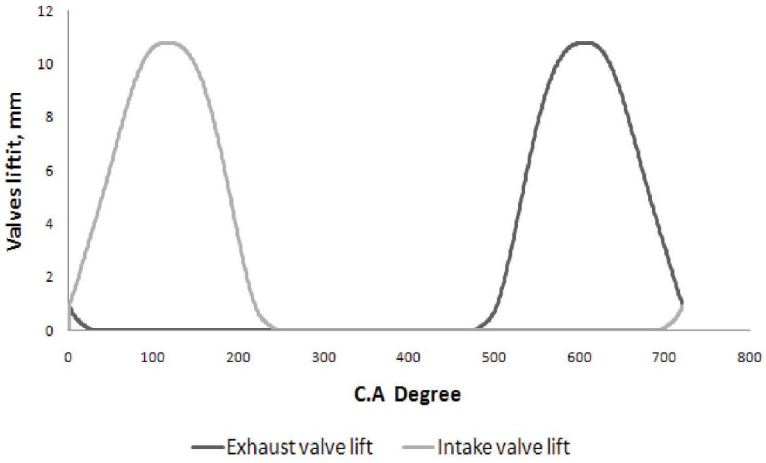

Fig. 7. Valve timing without scavenging

to see their sole effects on in-cylinder flow. Therefore effect of turbo-charging and scavenging on swirl and tumble formation can be investigated. Different valves timings are shown in Figs. 6 and 7, where in fig. 6 intake valves open at 80° BTDC and close at 44° ABDC and exhaust valves open at 80° BBDC and close at 76° ATDC resulting scavenging duration of 15° degrees. In Fig. 7 there is no valve overlap and only the effect of turbocharger is investigated.

Fig. 8 shows the intake flow. The plane shown in this figure is a vertical plane crossing the cylinder centre and

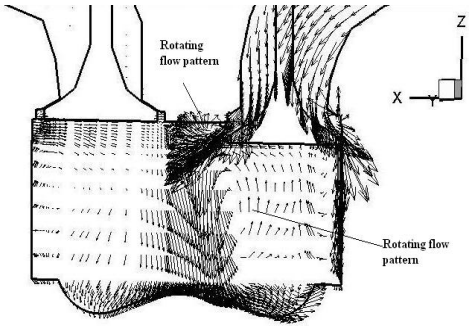

Fig. 8. Inlet flow of intake valves and port at 30° CA, as Predicted by KIVA3V2

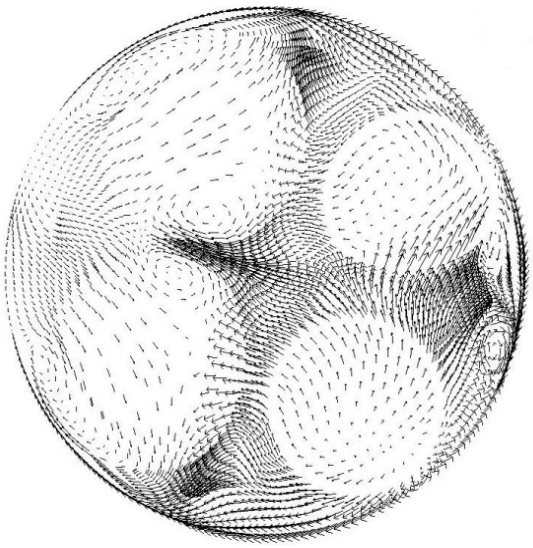

Fig. 9. Swirl formation predicted at plane z=19 by KIVA3V2

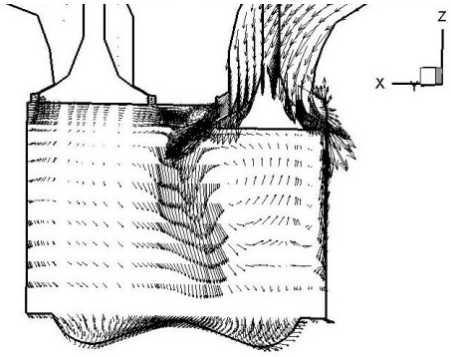

(a)

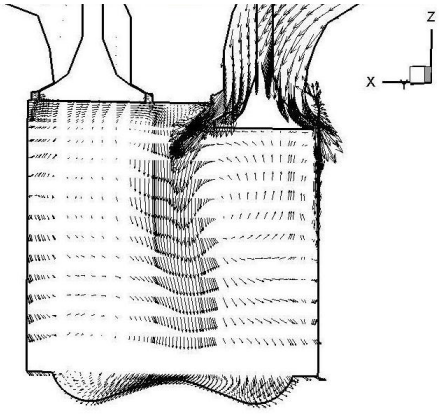

(b)

Fig. 10. Tumble formation process predicted at plane -145° by KIVA3V2 for (a) 60° CA and (b) 120° CA

the far valves centre. A significant large-scale rotating flow pattern is generated below the intake valves. Another weaker rotation pattern is also created below the cylinder head near the intake port, the direction of which is opposite to the main rotation pattern.

The swirl flow formation process is shown in Fig. 9 indicates a typical velocity vectors in a plane 19 cm, which is determined from BDC, below the cylinder head at 80° CA during intake stroke where the swirl ratio has the highest value.

The tumble flow formation process is shown in Fig. 10(a) during early stages of intake stroke where no apparent tumble flow is observed. However, as seen in Fig. 10 (b), farther down mid intake stroke, a tumble pattern is clearly visible. The tumble flow strengthens as air enters the cylinder during the filling process. By the end of intake process and into early stages of compression stroke, an organized tumble flow is clearly seen. Comparing Figs 10(a) and (b) and Fig. 8, it is concluded that the direction of the inlet flow at early intake stroke is different from that at the later stages. Later when tumble is formed, flow from under the valves is entrained. The intake flow follows the passage formed by the valves seat and its contour shown in Fig. 10(b).

Swirl ratio is shown in Fig. 11 for cases with and without turbo-charging together with any scavenging also the case with turbo-charging and scavenging. As shown turbocharger has huge effect on swirl ratio while the effect of scavenging becomes negligible when turbo-charging is used. In dual fuel engine natural gas is combined with air and mixture inters the cylinder. So during scavenging period mixture of fresh charge together with burnt gases can leave the cylinder with increased unburned hydrocarbon (UHC).

Fig. 11 shows turbo charging without scavenging there would be no major effect on swirl ratio and combustion, this would also eliminates the UHC. No turbo charging and scavenging results in low swirl ratio also it is shown that turbo charging and scavenging has major effects on in cylinder turbulent kinetic energy (Fig. 12).

Effects of turbo charging and scavenging on angular momentum are shown in figures 13 through 15. Again major effects of turbo-charging are clear through intake stroke where scavenging in earlier stages has huge effect on angular momentum.

Figs. 16 and 17 show the average turbulent kinetic energy k and its dissipation rate ε versus crank angle

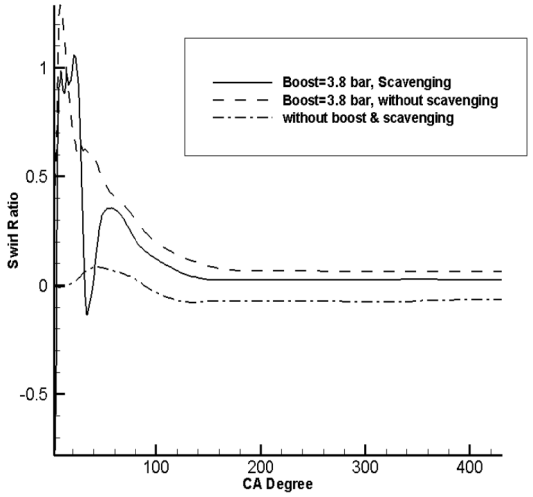

Fig. 11. Effects of turbo charging and scavenging on swirl ratio using KIVA3V2

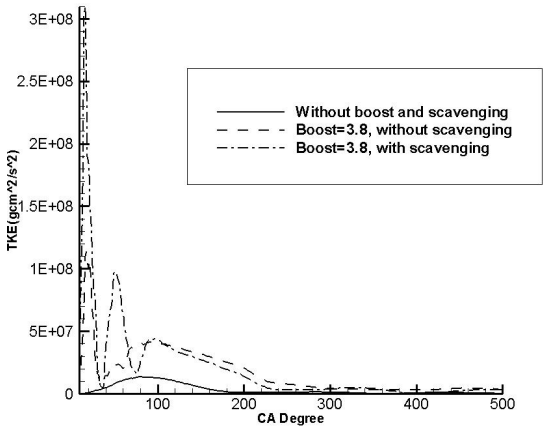

Fig. 12. Effects of turbo charging and scavenging on turbulent kinetic energy using KIVA3V2

with no boost and scavenging, respectively. Results are validated by experimental data available in reference [17]. The good agreement between numerical investigation and experimental data is clear. There are two turbulent kinetic energy peaks visible in fig.16. The first peak appears during the intake stroke, and is related to turbulence generated due to air flow through the intake valves.

It is important to note the increase in turbulent kinetic energy at the end of the compression stroke. The enhanced turbulent kinetic energy at that time is important to achieve good ignition and rapid flame propagation. It is apparent that there is a correlation between the break-up of tumble and the enhanced turbulent kinetic energy towards the end of compression stroke by comparing Figs 16 and 18. Examining above Figures it can be seen that the turbulent kinetic energy generated during intake stroke decays rapidly due to wall interaction at early stages of compression stroke.

As the piston moves further up during compression stroke, the tumble is squeezed into a smaller space leading to further turbulent kinetic energy generation where tumble is still noticeable. At 340° CA, the tumble is partially broken up although the velocity

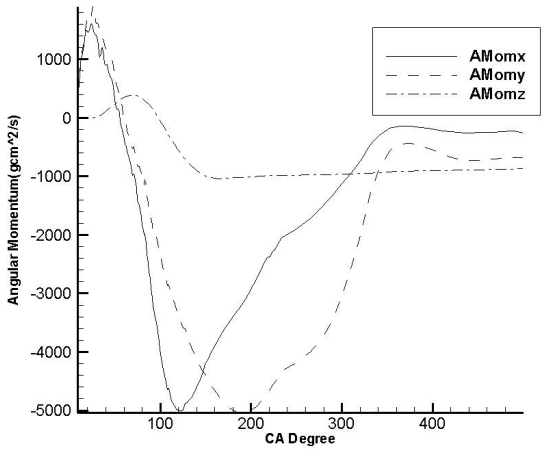

Fig. 13. Predicted angular momentum in three directions with no boost and scavenging

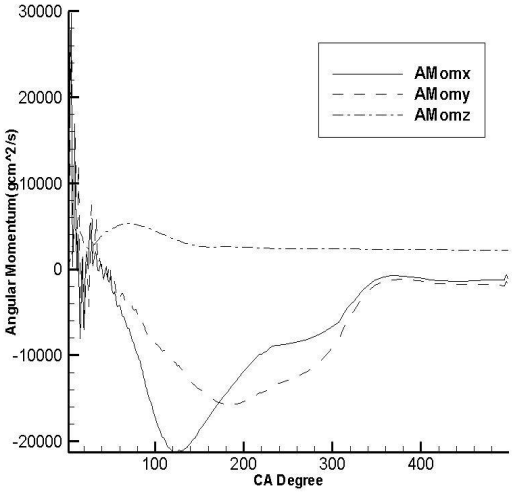

Fig. 14. Predicted angular momentum in three directions with boost=3.8 bar and no scavenging

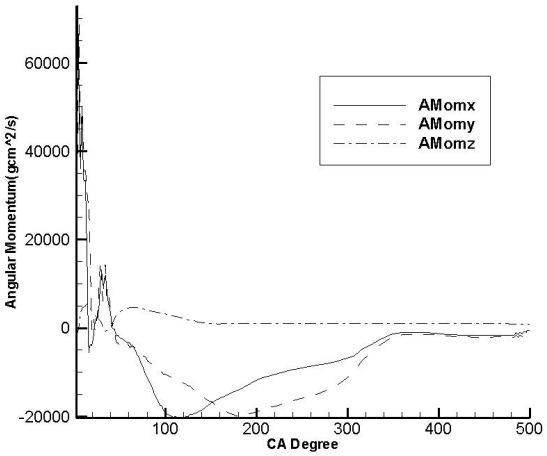

Fig. 15. Predicted angular momentum in three directions with boost=3.8 bar and scavenging

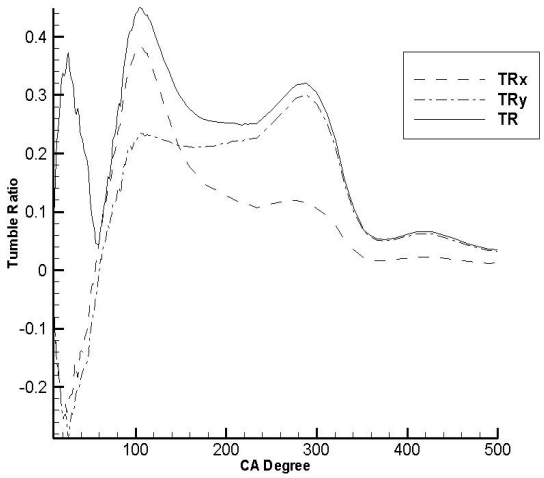

Fig. 18. Tumble ratio predicted by KIVA3V2

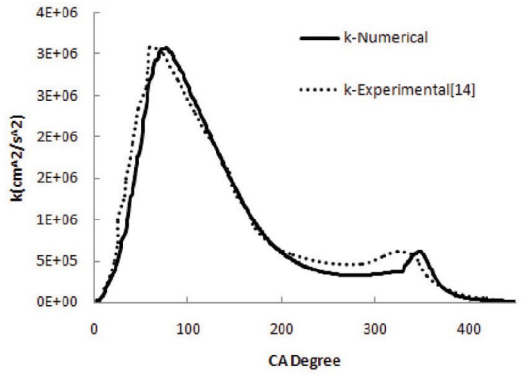

Fig. 16. Average turbulence kinetic energy k (Numerical and Experimental [17])

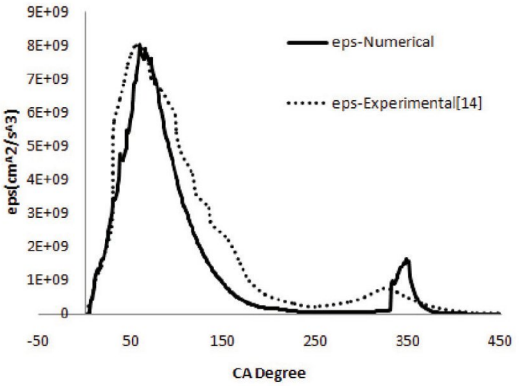

Fig. 17. Average turbulence kinetic dissipation rate (Numerical and Experimental [17])

gradient in the cylinder has increased. This results in a huge increase in turbulent kinetic energy causing the second peak relevant to figure 16.

6. CONCLUSIONS

The governing Navier–Stokes equations for three-dimensional unsteady turbulent compressible flow are developed and solved using KIVA3V2 to investigate intake and in-cylinder flow field of a four-valve dual fuel (natural gas/diesel oil) engine with following points:

1. The swirl ratio and tumble ratio is low for the newly developed dual fuel heavy duty diesel engine with its especial intake port configuration without turbo charging and excess valve overlapping effects.
2. The turbo-charging has a major effect on flow characteristics such as swirl ratio, turbulent kinetic energy and angular momentum. Turbo-charging maximizes the swirl ratio at least five times. Together with scavenging enhances the swirl ratio further more to six times. The angular momentum would improve drastically about sixty times
3. The combustion modeling which its results are not brought here due to lack of space confirm the fact that swirl ratio, turbulent kinetic energy and angular momentum have a major effect on combustion process and improved mixture

quality this could lead to an increase in the percentage use of natural gas with reduced engine emission levels and fuel economy.

REFERENCES

[1] R. G. Papagiannakis, D. T. Hountalas, C. D. Rakopoulos, D. C. Rakopoulos,"Combustion and performance characteristics of a DI diesel engine operating from low to high natural gas supplement ratios at various operating condition",SAE paper, NO 2008-01-1329

[2] Kouremenos D.A. and Rakopoulos C.D., "The operation of a turbulence chamber diesel engine, with LPG fumigation, for exhaust emissions control", VDI Forschung im Ingenieurwesen, Vol. 52, pp. 185-190, 1986.

[3] Stone C. R., Gould J. and Ladommatos N., "Analysis of bio-gas combustion in spark-ignition engines, by means of experimental data and a computer Simulation", J. of the Institute of Energy, Vol. 66, pp.180-187, 1993.

[4] Karim G. A., "A review of combustion processes in the dual fuel engine – the gas diesel engine", Progress in Energy and Combustion Science, Vol. 6, pp. 277-285, 1980.

[5] Stephenson, P. W. and Rutland, C. J. modeling the effects of intake flow characteristics on diesel engine combustion. SAE paper 950282, 1995.

[6] McLandress, A., Emerson, R., McDowell, P., and Rutland, C. Intake and in-cylinder ?ow modeling characterization of mixing and comparison with flow bench results. SAE paper 960635, 1996.

[7] C. L. Myung, K. H. Choi, I. G. Hwang, K. H. Lee and S. Park, "Effects of Valve Timing and Intake Flow Motion Control on Combustion and Time-Resolved HC & NOx Formation Characteristics", J. Automobile Engineering, 2009,161-169

[8] Amsden, A. A., O'Rourke, T.D. and Butler, T.D., 1989, "KIVA 2, a computer program for chemically reactive flows with sprays", Los Alamos National Laboratory report, LA-I 1560-MS, Los Alamos (USA).

[9] ANSYS ICEM CFD Engineering, 2002, "ANSYS ICEM CFD Users Manual".

[10] Khalil, E. B. and Karim, G. A. (2002), "A Kinetic Investigation of the Role of Changes in the Composition of Natural Gas in Engine Applications", Transaction of the ASME, Vol. 124, pp. 404-411

[11] Kong, S. C., Ayoub, N., and Reitz, R. D. (1992), "Modeling Combustion in Compression Ignition Homogeneous Charge Engines", SAE 920512.

[12] Kong, S. C., Han, Z., and Reitz, R. D., "The Development and Application of a Diesel Ignition and Combustion Model for Multidimensional Engine Simulation", SAE 950278.

[13] Rente, T., Golovichev, V. I., and Denbratt, I. (2001), "Effect of Injection Parameters on Auto-ignition and Soot Formation in Diesel Sprays", SAE 2001-01-3687.

[14] Launder, B. E. and Spalding, D. B. (1972), "Mathematical Models of Turbulence", Academic Press, New York.

[15] Stull, D. R. and Prophet, H. (1971), "JANAF Thermo chemical Tables", 2nd Ed. (U.S. Department of Commerce/National Bureau of Standards, NSRDS-NBS 37, June 1971).

[16] Han, Z. and Reitz, R. D. Turbulence modeling of internal combustion engines using RNG k–e models. Combust. Sci. and Technol., 1995, 106.

[17] Micklow, G. J., W- D., Gong. , "Intake and in cylinder flow field modeling of a four-valve diesel engine", J. Automobile Engineering, 2007,221

Nomenclature

B	bore (mm)
k	turbulence kinetics energy
N	engine speed
P	absolute pressure (kPa)
Q	heat transfer
Q_c	source due to chemical heat release
S	stroke (mm)
SW	initial swirl ratio
T	tumble ratio, temperature (K)
ρ	mass density of species m
Wm	molecular weight of species m
ε	dissipation of turbulence kinetics energy

Abbreviation

ABDC	after bottom dead center
ATDC	after top dead center
BBDC	before bottom dead center
BTDC	before top dead center
CA	crank angle
CFD	computational fluid dynamic
CIDI	compression ignition direct injection
EVC	exhaust valve closing
EVO	exhaust valve opening
IVC	intake valve closing
IVO	intake valve opening
LPG	liquefied petroleum gas
PSR	perfectly stirred reactor
TDC	top dead center
UHC	unburned hydrocarbon